Rim-Integrated Bluetooth Antenna for Smartwatches with Full-Metallic Structure

Ali Kourani*, Sihan Shao*, Mohamed Räsänen*, Jan Bergman*, Rasmus Luomaniemi†, Jari Holopainen*
*Department of Electronics and Nanoengineering, Aalto University School of Electrical Engineering, Espoo, Finland
Radientum Oy, Tampere, Finland
E-mail: ali.kourani@aalto.fi, rasmus.luomaniemi@radientum.fi

***Abstract*—The integration of smart technology into wearable devices has been rapidly evolving, leading to the proliferation of smartwatches, fitness trackers, smart jewelry, and other connected accessories that blend functionality with everyday use. As these devices become increasingly compact, efficient, and sophisticated, the design of internal components, such as antennas, plays a critical role in optimizing performance. This paper explores the design, manufacturing, and prototype measurements of a Bluetooth antenna integrated into the metallic rim of a smartwatch. By embedding the antenna within the structural elements of the device, we address challenges related to space constraints, complicated metallic structure inside the smartwatch influencing the antenna pattern, and overall device aesthetics. The measured prototype showed a −10 dB impedance bandwidth over the 2.38–2.65 GHz frequency range, which encompasses 2.4–2.5 GHz range of interest, when measured on a human tissue phantom, with a total efficiency of 30%.**

***Index Terms*—Bluetooth, Wearable Antenna, Small Antenna, Slot Antenna, Smartwatch.**

I. Introduction

Antennas for body-area applications have become an integral part of modern life, offering users convenient and constant access to information, communication, and health monitoring [1]–[3]. Among the most popular wearable devices are smartwatches, which combine the functionality of traditional timepieces with the capabilities of smartphones. These devices rely heavily on wireless communication protocols, such as Bluetooth, to connect with other devices, transfer data, and provide a seamless user experience.

As the demand for smaller and more aesthetically pleasing smartwatches continues to grow, the integration of components such as antennas becomes challenging. The challenges include the influence of metallic structure on the radiation pattern of the antenna. This is besides the significant influence imposed by the contact between the wearable structure and the human skin. The goal in the design process would be to maintain impedance matching across the frequency band of interest besides a low directivity of the antenna in a metallic stricture and when it is in contact with human skin.

Several works in the literature have addressed antenna designs where the structure is in contact with human skin [3]–[7], while others have considered the integration of antennas into the metallic structures of the final product [6], [8]. Although these studies provide some proof-of-concept designs, many lack prototype measurements, and some do not account for a fully metallic structure. Our work proposes a proof-of-concept design, accompanied by prototype measurements with a human tissue phantom, for a fully metallic smartwatch structure. This design takes into consideration other internal components such as the battery, PCB for electronic components, touch screen, and metallic base of the smartwatch.

The rest of this paper is organized as follows. Section II details the design of the smartwatch structure integrating the antenna into its metallic rim. Section III describes the measurement results and some performance evaluation of the manufactured prototype. The paper concludes in Section IV.

II. Structure Design

A. Smartwatch Design

The smartwatch prototype design comprises several components, as illustrated in Fig. 1. The chassis of the smartwatch is modeled using a plastic structure with electrical parameters as $\varepsilon_r = 3$ and $\tan\delta = 0.0031$ designed in CST Studio Suite. To closely replicate a realistic structure, the display was modeled as a copper sheet covering the entire top face of the smartwatch. Inside the plastic chassis, a copper block, measuring $25 \times 25 \times 5$ mm^3, was added to represent the battery. Additionally, a printed circuit board (PCB) with dimensions of $32 \times 30 \times 1.5$ mm^3 was incorporated. This PCB hosts other electronic components and is utilized to solder the matching circuit critical for our design.

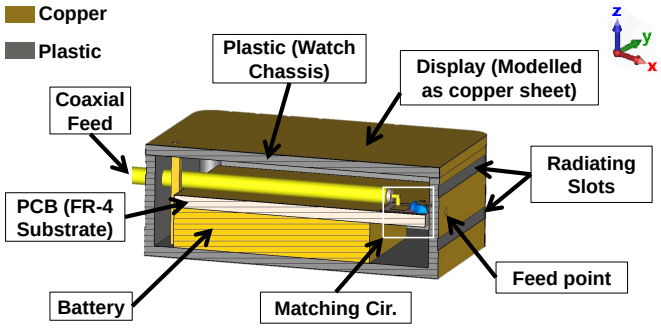

Fig. 1. The xz-cross section view of the smartwatch structure.

B. Antenna Design

The target design relies on incorporating slots into the metallic rim of the smartwatch, which function as slot antennas. A copper wire connects the matching circuit to the

center point of the lateral copper face of the watch in the positive x-direction. To maintain a symmetrical aesthetic, the four lateral faces of the watch are designed to be identical. Fig. 2 describes the dimensions adopted for the final design.

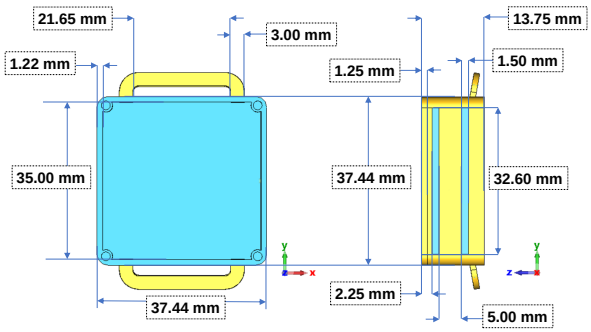

Fig. 2. Major dimensions of the smartwatch design: top view (left) with the display part removed and side view (right) with the display.

C. Matching Circuit

The S11 parameters of the design were exported to AWR Microwave Office to design a matching circuit with realistic components. The chosen topology for the matching circuit is a series capacitor and shunt inductor from the coaxial feed towards the antenna feed point. The components are $C_1 = 0.6$ pF and $L_1 = 3.6$ nH.

1) Matching Components Tolerance Study: To account for possible uncertainties in the matching components, a parametric sweep was conducted on the capacitor value to study the effect of its tolerance on the matching, as reported in Fig. 3. This parametric study demonstrated that a tolerance of 0.1pF would still maintain effective matching across the 2.4–2.5 GHz frequency band.

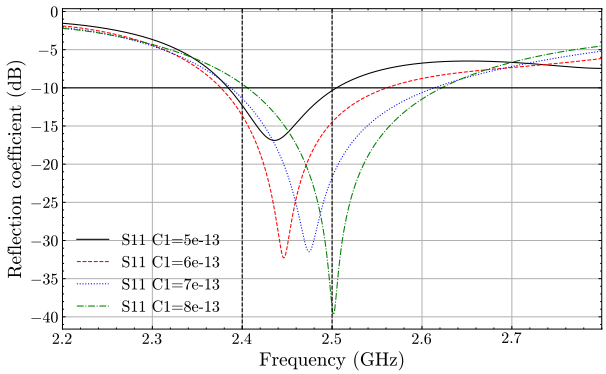

Fig. 3. Effect of the capacitor value tolerance on the reflection coefficient.

D. Critical Design Observations

1) Grounding Structure: As part of the design, the antenna was grounded to the battery ground, and a grounding element, as indicated in Fig. 1, was integrated into the final design. This element makes contact with the display metallization, the outer conductor of the coaxial feed, the PCB ground plane, the lower face metallization, and the battery. The lateral face metallizations also connect with both the display and lower face metallizations. The critical role of this grounding structure became evident when its height was adjusted to no longer touch either the display or the lower conductor, given that both the display and bottom metallizations are interconnected through the corner metallizations. This adjustment, which alters the current distribution, led to a drastic change in the resonance frequency.

2) Distance between Ground Plane and Chassis wall: Another important observation noticed while tweaking the design parameters to see which could have a significant influenced on the resonance frequency if varied during manufacturing was the distance of separation between the PCB (ground plane) and the wall of the chassis. The impact is reported in Fig. 4 showing a drastic change in the reflection coefficient once the PCB is brought away from the chassis wall with the feed point.

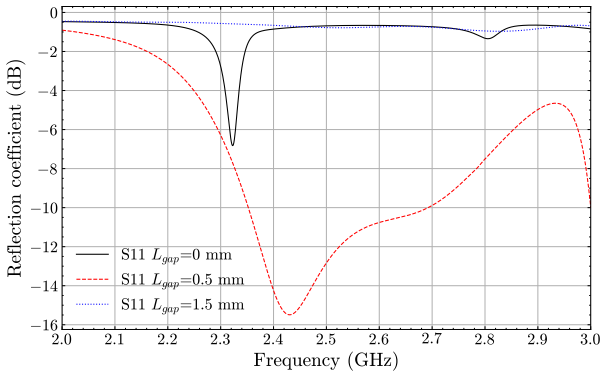

Fig. 4. Reflection coefficient simulation for different distance of separation (L_{gap}) between the PCB and chassis wall in the positive x-direction face.

III. Results and Performance Analysis

A. Prototype Manufacturing

The final prototype was manufactured by 3D printing the smartwatch chassis from plastic. The coaxial feed was inserted from the negative x-direction lateral face and soldered to the ground plane of the PCB. The matching circuit was also soldered onto the PCB, with a feed wire connecting it to the feed point at the center of the positive x-direction lateral face. The metallization of the surfaces was achieved using copper tape, applied as accurately as possible to match the dimensions of the slots. Fig. 5 illustrates various manufacturing stages and the final appearance of the prototype.

B. Prototype Evaluation: Simulation vs Measurement

Reflection coefficient measurements were conducted using a vector network analyzer (VNA) in the laboratory, with absorbers surrounding the prototype to isolate reflections, as depicted in Fig. 5. For the measurements involving a human phantom, the prototype was positioned on a $5 \times 5 \times 5\,\text{cm}^3$ cube made of a material that mimics the electrical properties of human tissue. The human tissue phantom has the electrical parameters as $\varepsilon_r = 28$, $\sigma = 0.62$ S/m. This setup helps in

assessing how the device performs in conditions that closely resemble its intended use on a human body. Fig. 6 presents plots of the simulated and measured reflection coefficients in free space (FS), with a human tissue phantom, and with an actual human wrist. The measured reflection coefficient yields promising results, as the human tissue phantom measurements demonstrate a −10 dB impedance bandwidth of 2.39–2.6 GHz encompassing the 2.4–2.5 GHz band of interest.

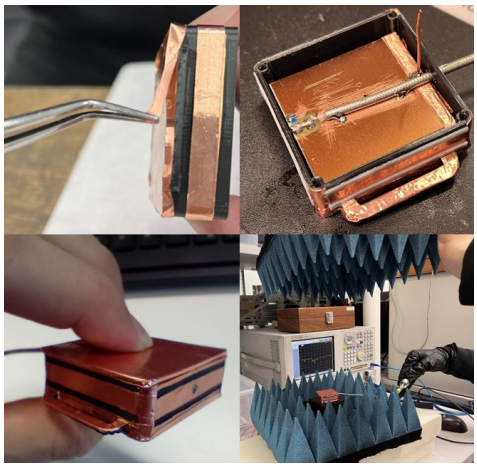

Fig. 5. Manufacturing stages,the final prototype, and the reflection coefficient measurement process.

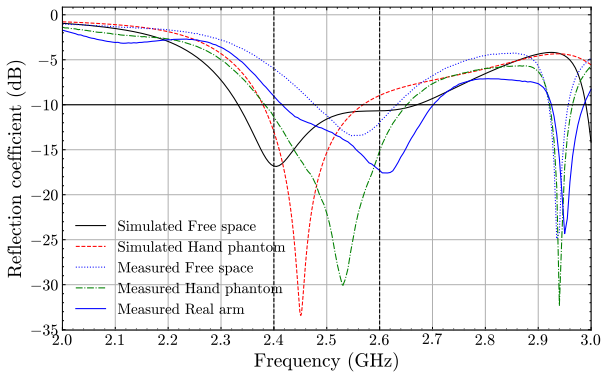

Fig. 6. Simulated and measured frequency response of the reflection coefficient of the designed prototype.

The far-field radiation pattern and radiation efficiency were measured using the MVG StarLab 6 GHz antenna measurement system. Fig. 7 demonstrates the simulated realized gain pattern for both free space (FS) and human tissue phantom (HP) cases, while Fig. 8 presents the measured realized gain pattern. For a more precise comparison, Fig. 9 depicts the major cuts at $\phi = 0^\circ$ and $\phi = 90^\circ$, corresponding to the xz-plane and yz-plane, respectively. Table I summarizes a metric comparison between the simulated and measured results for the design in the human tissue phantom case.

The results show a similar far-field pattern with a bit of ripples in the measured one, which could be caused by the bending of the coaxial feed near the prototype during measurement. The total efficiency measured at 2.45 GHz

TABLE I
SIMULATION VS MEASUREMENT RESULTS WITH HUMAN TISSUE PHANTOM AT 2.45 GHZ

	Imp. BW (GHz)	Real. Gain	Total Eff.	Directivity
Sim. HF	2.38–2.57	−0.37 dBi	50%	2.64
Meas. HF	2.38–2.65	−1 dBi	34%	3.68

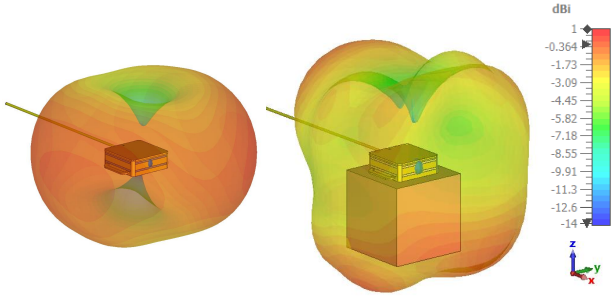

Fig. 7. Simulated realized gain pattern at 2.45 GHz.

dropped by 16 percentage points. This significant decrease in total efficiency is likely caused by inaccuracies in the electrical parameters used in simulations, particularly the loss tangent of the plastic chassis of the watch. Additionally, manufacturing imperfections and the use of copper tape for metallization, which introduces numerous bends and artifacts, likely contribute to increased Ohmic losses. The directivity results look promising as both the simulation and measurement show relatively low directivity with a slight increase in the measurement. Low directivity is important to ensure that the smartwatch antenna would radiate almost equally in all directions, which would help in communicating with access points no matter where it is placed.

C. Performance Study and Comparison to Work in Literature:

To evaluate the performance of the manufactured prototype in terms of Bluetooth communication range, we set a goal of 10 m coverage distance. Assuming an access point with a receiver gain of 0 dB and a required received power of −70 dBm, we calculate the required realized gain to achieve that target coverage distance using Friis equation:

$$P_r = P_t + G_t + G_r - 20\log_{10}(d) - 20\log_{10}(f) - 20\log_{10}\left(\frac{4\pi}{c}\right)$$

where P_r represents the received power, which is −70 dBm. The transmitted power, P_t, is assumed to be 0 dBm. Both G_t and G_r are the gains of the transmitter and receiver in dB-scale, respectively. The distance between the transmitter and receiver, d, is 10 m, while the operating frequency, f, is 2.45 GHz and c is the speed of light in vacuum.

Solving the Friis equation for the required realized gain of the smartwatch antenna, G_t, results in a −9.7 dB gain needed to cover 10 m distance. Comparing this result to the measured realized gain pattern of the prototype, we observe that the antenna achieves gains sufficient to meet this requirement within a wide angular range, specifically, for elevation

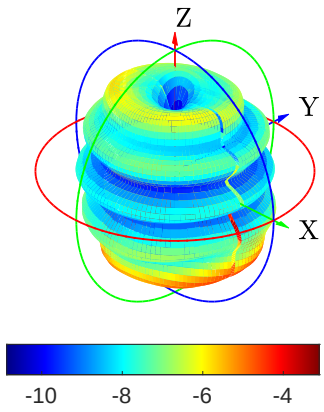

Fig. 8. Measured realized gain pattern at 2.45 GHz with human tissue phantom.

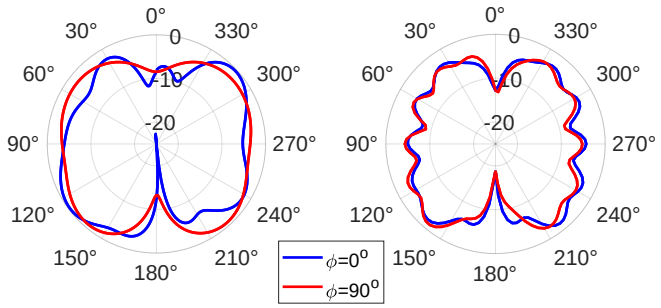

Fig. 9. Major cuts of the simulated (left) and measured (right) realized gain patterns in dB-scale with human tissue phantom.

angles θ between 6° and 168°, meaning that the antenna can maintain reliable Bluetooth communication within this angular range when the smartwatch is worn on the wrist. This result highlights the effectiveness of the antenna design.

The wide angular coverage provided by the low directivity of the antenna design is critical for maintaining communication regardless of the orientation of the smartwatch relative to the access point. This feature ensures that the device can reliably communicate in various usage scenarios, making it suitable for practical applications in wearable technologies. Table II provides a short parametric comparison with 5 other designs of wearable smart device antennas at 2.45 GHz.

TABLE II
COMPARISON OF THE PROPOSED DESIGN WITH WEARABLE SMART DEVICE ANTENNAS AT 2.45 GHz

Antenna	Efficiency		Directivity with HP
	Sim. efficiency FS / HP	Meas. efficiency FS / HP	Sim. / Meas.
Proposed	68% /50%	N/A / 34%	2.64 dB / 3.68 dB
[4]	69% / 26%	N/A / N/A	4.96 dB / N/A
[7]	67% / 44%	61% / 36%	6.3 dB / 5.94 dB
[8]	90% / 70%	N/A / N/A	5.35 dB / N/A
[9]	81% / 80%	70% / 60%	5.87 dB / 4.94 dB
[10]	53% / 39%	50% / N/A	N/A / N/A

IV. CONCLUSIONS

In conclusion, this paper demonstrated the design, manufacturing, and performance evaluation of a Bluetooth antenna integrated into the metallic rim of a smartwatch. This approach addressed the key challenges faced in the development of wearable technologies, particularly in optimizing antenna performance while adopting a small, compact, fully metallic structure. Integrating the antenna into the metallic rim of the smartwatch not only helped in overcoming the detrimental effects of the metallic components on the radiation pattern of the antenna but also ensured the aesthetic design of the device. Our prototype measurements, conducted using a human tissue phantom, confirmed that the −10 dB impedance bandwidth encompasses the 2.4–2.5 GHz frequency range, with total efficiency of 30%. The prototype measurement results demonstrated a wide angular coverage of a target 10 m distance provided by the low directivity of the antenna design. Future work could focus on further refining the antenna design to enhance its bandwidth and efficiency.

ACKNOWLEDGEMENT

The authors would like to acknowledge Aalto electronics ICT (AELICT) for access to microwave instruments and the MVG StarLab 6 GHz antenna measurement facility.

REFERENCES

[1] A. Kiourti, "Rfid antennas for body-area applications: From wearables to implants," *IEEE Antennas and Propagation Magazine*, vol. 60, no. 5, pp. 14–25, 2018.

[2] H. Sun, Z. Zhang, R. Q. Hu, and Y. Qian, "Wearable communications in 5g: Challenges and enabling technologies," *IEEE Vehicular Technology Magazine*, vol. 13, no. 3, pp. 100–109, 2018.

[3] A. K. Arya, T. Kim, H. Kim, J. Oh, J. Kim, D. Moon, and S. Kim, "Compact ble antenna with a modified pifa configuration for wearable emg monitor," *IEEE Sensors Journal*, vol. 23, no. 15, pp. 17 648–17 655, 2023.

[4] S.-W. Su and Y.-T. Hsieh, "Integrated metal-frame antenna for smartwatch wearable device," *IEEE Transactions on Antennas and Propagation*, vol. 63, no. 7, pp. 3301–3305, 2015.

[5] J. Zhang, B. Wang, S. Yan, and J. Zhang, "Design of button antenna for wearable applications in bluetooth band," in *2024 IEEE International Workshop on Radio Frequency and Antenna Technologies (iWRFAT)*, 2024, pp. 127–129.

[6] Y.-Y. Yang and H.-D. Chen, "Open slot antenna for smartwatch application," in *2016 IEEE 5th Asia-Pacific Conference on Antennas and Propagation (APCAP)*, 2016, pp. 41–42.

[7] R. Luomaniemi, C. Cziezerski, H. Mäki, J. Holopainen, and V. Viikari, "Bluetooth antenna for smart jewellery with metal covers," in *2019 13th European Conference on Antennas and Propagation (EuCAP)*, 2019, pp. 1–4.

[8] D. Wu, S. W. Cheung, Q. L. Li, and T. I. Yuk, "Slot antenna for all-metal smartwatch applications," in *2016 10th European Conference on Antennas and Propagation (EuCAP)*, 2016, pp. 1–4.

[9] D. Wu and S. W. Cheung, "A cavity-backed annular slot antenna with high efficiency for smartwatches with metallic housing," *IEEE Transactions on Antennas and Propagation*, vol. 65, no. 7, pp. 3756–3761, 2017.

[10] Y.-S. Chen and T.-Y. Ku, "A low-profile wearable antenna using a miniature high impedance surface for smartwatch applications," *IEEE Antennas and Wireless Propagation Letters*, vol. 15, pp. 1144–1147, 2016.